2:1 Resonance in the delayed nonlinear Mathieu equation

Tina M. Morrison · Richard H. Rand

Abstract We investigate the dynamics of a delayed nonlinear Mathieu equation:

$$\ddot{x} + (\delta + \varepsilon\alpha\,\cos t)x + \varepsilon\gamma x^3 = \varepsilon\beta x(t - T)$$

in the neighborhood of $\delta = 1/4$. Three different phenomena are combined in this system: 2:1 parametric resonance, cubic nonlinearity, and delay. The method of averaging (valid for small ε) is used to obtain a slow flow that is analyzed for stability and bifurcations. We show that the 2:1 instability region associated with parametric excitation can be eliminated for sufficiently large delay amplitudes β, and for appropriately chosen time delays T. We also show that adding delay to an undamped parametrically excited system may introduce effective damping.

Keywords Averaging · Degenerate Hopf · Delay · Nonlinear Mathieu · Parametric excitation

1 Introduction

This paper concerns the dynamics of the following parametrically excited, nonlinear differential delay equation (DDE)

$$\ddot{x}(t) + (\delta + a\cos t)x(t) + cx(t)^3 = bx(t - T) \quad (1)$$

T. M. Morrison · R. H. Rand (✉)
Department of Theoretical and Applied Mechanics, Cornell University, Ithaca, NY 14853, USA
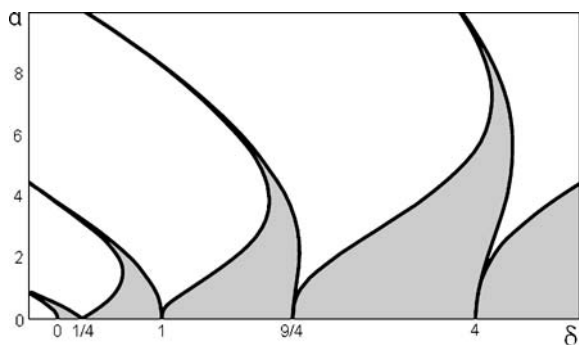e-mail: rhr2@cornell.edu

where δ, a, b, c, and T are parameters: δ is the frequency squared of the simple harmonic oscillator, a is the amplitude of the parametric resonance, b is the amplitude of delay, c is the amplitude of the cubic nonlinearity, and T is the time delay. Equation (1) is a model for high-speed milling: "High-speed milling is a kind of parametrically interrupted cutting as opposed to the self-interrupted cutting arising in unstable turning processes." [1]. See, e.g., [2, 3].

Various special cases of Equation (1) have been studied by others, depending on which parameters are zero. In the case that b and c are zero, we have the linear Mathieu equation, the stability chart for which is well known [4], see Fig. 1. In the case that only b is zero, we have a nonlinear Mathieu equation for which the bifurcations associated with stability change are also well known [4]. In the case that a and c are zero, we have the linear autonomous DDE of Bhatt and Hsu [5], who generated stability charts for various delay parameters. Figure 2 is the stability chart for Equation (1) with $a = c = 0$ and $T = 2\pi$.

The undamped linear form of Equation (1) was studied by Insperger and Stépán [6], who, by utilizing the method of exponential multipliers, generated the stability chart for a fixed time delay of $T = 2\pi$, see Fig. 3.

In this paper, we use the method of averaging [7] to generate stability charts and associated bifurcations for the delayed nonlinear Mathieu Equation (1) for a general time delay. We note that although DDE's are infinite dimensional [4], and hence more complicated than ODEs, a Taylor series expansion is used to replace

Fig. 1 Stability chart for the linear Mathieu Equation [4] without delay, Equation (1) with $b = c = 0$. The solution is stable in the shaded regions
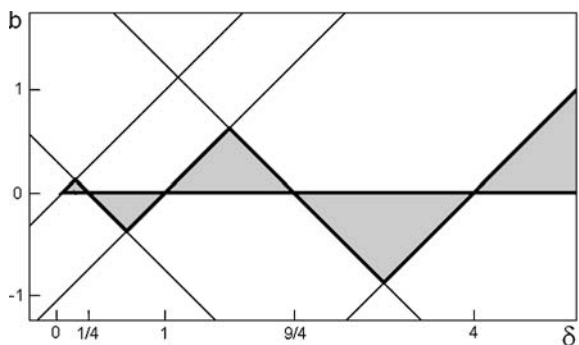

Fig. 2 Stability chart for the Hsu–Bhatt DDE [5], Equation (1) with $a = c = 0$ and $T = 2\pi$. The solution is stable in the *shaded regions*
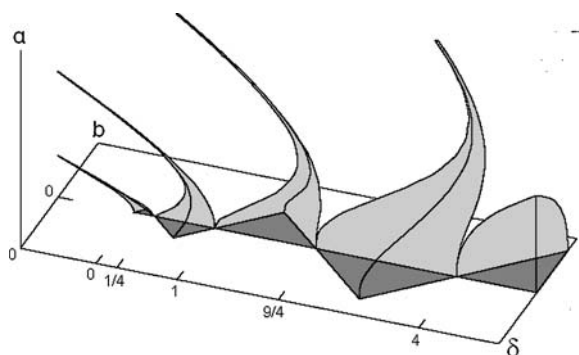

Fig. 3 Stability chart for the linear delayed Mathieu Equation [6] with $T = 2\pi$ and $c = 0$. The solutions in the *shaded regions* are stable. The *darker shaded triangles* are those of Fig. 2

the DDE slow flow with an ODE slow flow, an approximation that is valid for small εT. Stability charts for the linear delayed equation with general time delay were numerically generated by Breda et al. [8] and Insperger and Stépán [9].

2 Averaging

In preparation for averaging Equation (1), we introduce a small parameter ε by scaling $a = \varepsilon\alpha$, $b = \varepsilon\beta$, and $c = \varepsilon\gamma$. In addition, we detune off of 2:1 resonance by setting $\delta = 1/4 + \varepsilon\delta_1$

$$\ddot{x}(t) + \left(\frac{1}{4} + \varepsilon\delta_1 + \varepsilon\alpha\cos t\right)x(t) + \varepsilon\gamma x(t)^3$$
$$= \varepsilon\beta x(t - T). \tag{2}$$

When $\varepsilon = 0$, Equation (2) reduces to $\ddot{x} + x/4 = 0$, with the solution

$$x(t) = A\cos\left(\frac{t}{2} + \phi\right),$$
$$\dot{x}(t) = -\frac{A}{2}\sin\left(\frac{t}{2} + \phi\right). \tag{3}$$

For $\varepsilon > 0$, we look for a solution in the form of Equation (3) but treat A and ϕ as time dependent. Variation of parameters gives the following equations on $A(t)$ and $\phi(t)$

$$\dot{A}(t) = -2\varepsilon\sin\left(\frac{t}{2} + \phi\right)F\left(A\cos\left(\frac{t}{2} + \phi\right),\right.$$
$$\left.-\frac{A}{2}\sin\left(\frac{t}{2} + \phi\right), t\right) \tag{4}$$

$$\dot{\phi}(t) = -2\frac{\varepsilon}{A}\cos\left(\frac{t}{2} + \phi\right)F\left(A\cos\left(\frac{t}{2} + \phi\right),\right.$$
$$\left.-\frac{A}{2}\sin\left(\frac{t}{2} + \phi\right), t\right), \tag{5}$$

where $F(x, \dot{x}, t) = -(\delta_1 + \alpha\cos t)x(t) - \gamma x(t)^3 + \beta x(t - T)$ in which $x(t)$ is given by Equation (3). For small ε, we use the method of averaging [10], replacing the right-hand sides of Equations (4) and (5) by their averages over one 2π period of the forcing function $\cos t$

$$\dot{A} \approx -\frac{\varepsilon}{\pi}\int_0^{2\pi}\sin\left(\frac{t}{2} + \phi\right)F\,dt \tag{6}$$

$$\dot{\phi} \approx -\frac{1}{A}\frac{\varepsilon}{\pi}\int_0^{2\pi}\cos\left(\frac{t}{2} + \phi\right)F\,dt, \tag{7}$$

where

$$F = -(\delta_1 + \alpha \cos t) A \cos\left(\frac{t}{2} + \phi\right)$$

$$- \gamma A^3 \cos^3\left(\frac{t}{2} + \phi\right)$$

$$+ \beta A_{\mathrm{d}} \cos\left(\frac{1}{2}(t - T) + \phi_{\mathrm{d}}\right), \qquad (8)$$

where $A_{\mathrm{d}} = A(t - T)$ and $\phi_{\mathrm{d}} = \phi(t - T)$. Evaluating the integrals in Equations (6) and (7) gives

$$\dot{A} = \varepsilon\left(\frac{A\,\alpha\,\sin 2\phi}{2} - A_d\,\beta\,\sin\left(\frac{T}{2} - \phi_d + \phi\right)\right) \quad (9)$$

$$\dot{\phi} = \varepsilon\left(\frac{3\gamma\,A^2}{4} - \frac{A_d\,\beta\,\cos\left(\frac{T}{2} - \phi_d + \phi\right)}{A}\right.$$

$$\left. + \frac{\alpha\,\cos 2\phi}{2} + \delta_1\right)$$

$$(10)$$

Thus, $\dot{A}$ and $\dot{\phi}$ are $O(\varepsilon)$. We now Taylor expand A_d and ϕ_d

$$A_{\mathrm{d}} = A(t - T) = A(t) - T\dot{A}(t) + \frac{1}{2}T^2\ddot{A}(t) + \cdots$$

$$(11)$$

$$\phi_{\mathrm{d}} = \phi(t - T) = \phi(t) - T\dot{\phi}(t) + \frac{1}{2}T^2\ddot{\phi}(t) - \cdots$$

$$(12)$$

Thus, we can replace A_{d} and ϕ_{d} by $A(t)$ and $\phi(t)$ in Equations (9) and (10) since $\dot{A}$ and $\dot{\phi}$ and $\ddot{A}$ and $\ddot{\phi}$ are of $O(\varepsilon)$ and $O(\varepsilon^2)$, respectively [11]. This approximation reduces the infinite-dimensional problem into a finite-dimensional problem by assuming εT is small.

After substituting the above approximation into Equations (9) and (10), we obtain

$$A' = A\left(\frac{\alpha}{2}\sin 2\phi - \beta\sin\frac{T}{2}\right) \qquad (13)$$

$$\phi' = \frac{3\gamma}{4}A^2 + \frac{\alpha}{2}\cos 2\phi - \beta\cos\frac{T}{2} + \delta_1, \qquad (14)$$

where primes represent differentiation with respect to *slow time* $\eta = \varepsilon t$. We may obtain an alternate form of the slow flow Equations (13) and (14) by transforming from polar coordinates A and ϕ to rectangular coordinates u and v via $u = A\cos\phi$, $v = -A\sin\phi$, giving

$$u' = -\left(\beta\sin\frac{T}{2}\right)u + \left(\delta_1 - \frac{\alpha}{2} - \beta\cos\frac{T}{2}\right)v$$

$$+ \frac{3\gamma}{4}v(u^2 + v^2). \qquad (15)$$

$$v' = \left(-\delta_1 - \frac{\alpha}{2} + \beta\cos\frac{T}{2}\right)u - \left(\beta\sin\frac{T}{2}\right)v$$

$$- \frac{3\gamma}{4}u(u^2 + v^2) \qquad (16)$$

Note that from Equation (3), we have

$$x(t) = A\cos\left(\frac{t}{2} + \phi\right) = A\cos\phi\,\cos\frac{t}{2}$$

$$- A\sin\phi\,\sin\frac{t}{2} = u\cos\frac{t}{2} + v\sin\frac{t}{2}. \qquad (17)$$

3 Slow flow equilibria: Stability and bifurcation

From Equation (17), we see that in general an equilibrium point in the slow flow (13) and (14) or (15) and (16) corresponds to a periodic motion in the original system (2). The origin $u = v = 0$ is an exception since it is an equilibrium point in both the slow flow equations and in the original system.

In order to find slow flow equilibrium points, we set $A' = \phi' = 0$ in Equations (13) and (14), and utilize the trig identity $\sin^2 2\phi + \cos^2 2\phi = 1$ to obtain the following condition on R, where $R = A^2$,

$$9\gamma^2 R^2 + 24\gamma\left(\delta_1 - \beta\cos\frac{T}{2}\right)R$$

$$+ 4\left(4\beta^2 - \alpha^2 + 4\delta_1^2 - 8\beta\delta_1\cos\frac{T}{2}\right) = 0. \qquad (18)$$

Equation (18) is a quadratic on R. The two solutions are

$$R = \frac{4}{3\gamma}\left[\beta\cos\frac{T}{2} - \delta_1 \pm \frac{1}{2}\sqrt{\alpha^2 - 4\beta^2\sin^2\frac{T}{2}}\right]. \qquad (19)$$

Each value of R corresponds to two nontrivial slow flow equilibria located 180° apart. This may be seen by noting that Equations (15) and (16) are invariant under the transformation $(u, v) \mapsto (-u, -v)$, which means that if (u, v) is a slow flow equibrium, then so is $(-u, -v)$.

R must be nonnegative for nontrivial equilibrium points. This condition yields two inequalities

$$\delta_1 \leq \beta \cos \frac{T}{2} \pm \frac{1}{2}\sqrt{\alpha^2 - 4\beta^2 \sin^2 \frac{T}{2}}. \qquad (20)$$

And for real roots, the discriminant in the inequality in Equation (20) must be positive. This condition yields

$$\left| \sin \frac{T}{2} \right| \leq \frac{1}{2} \left| \frac{\alpha}{\beta} \right|. \qquad (21)$$

Hence, for a given α and β, the inequality (21) gives a condition on the time delay T such that there will exist nontrivial slow flow equilibrium points. In the case that $|\beta/\alpha| \leq 1/2$, there will exist nontrivial fixed points for all T.

When the inequality in Equation (21) is satisfied, there are at least *two* nontrivial slow flow equilibrium points if,

$$\delta_1 < \beta \cos \frac{T}{2} + \frac{1}{2}\sqrt{\alpha^2 - 4\beta^2 \sin^2 \frac{T}{2}}. \qquad (22)$$

In addition, there will be *two* more nontrivial slow flow equilibrium points if,

$$\delta_1 < \beta \cos \frac{T}{2} - \frac{1}{2}\sqrt{\alpha^2 - 4\beta^2 \sin^2 \frac{T}{2}}. \qquad (23)$$

Thus, it is possible to have up to four nontrivial slow flow equilibria. When we include the origin, this makes a possible total of up to five slow flow equilibria. Next, we investigate which parameter combinations of δ_1 and T cause the slow flow equilibrium points to change stability for a given α and β, and which bifurcations, if any, accompany the change in stability.

The *trace* and *determinant* of the Jacobian matrix evaluated at an equilibrium point contain the local stability information. Recall that a saddle-node or pitchfork bifurcation generically occurs when the $\text{Det}(J) = 0$, and a Hopf bifurcation generically occurs when the $\text{Tr}(J) = 0$ and $\text{Det}(J) > 0$ [12]. From the

slow flow Equations (15) and (16), the Jacobian matrix is

$$J = \begin{bmatrix} -\beta \sin \frac{T}{2} + \frac{3\gamma}{2}uv & \delta_1 - \frac{\alpha}{2} - \beta \cos \frac{T}{2} \\ & + \frac{3\gamma}{4}u^2 + \frac{9\gamma}{4}v^2 \\ -\delta_1 - \frac{\alpha}{2} + \beta \cos \frac{T}{2} & \\ -\frac{3\gamma}{4}v^2 - \frac{9\gamma}{4}u^2 & -\beta \sin \frac{T}{2} - \frac{3\gamma}{2}uv \end{bmatrix}, \qquad (24)$$

where u and v are to be evaluated at the slow flow equilibria.

The trace of the Jacobian matrix is

$$\text{Tr}(J) = -2\beta \sin \frac{T}{2}. \qquad (25)$$

Note that $\text{Tr}(J)$ is a function of the delay parameters only, and in particular does not depend on R. Therefore, $\text{Tr}(J) = 0$ at *all* of the slow flow equilibrium points when $\beta = 0$, $T = 0$, or $T = 2\pi$. In particular, a change of stability and a possible Hopf bifurcation (birth of a limit cycle) will occur at $T = 2\pi$ if $\text{Det}(J) > 0$.

The determinant of the Jacobian matrix is

$$\text{Det}(J) = \frac{27}{16}\gamma^2 R^2 - 3\gamma \left(\beta \cos \frac{T}{2} - \delta_1 \right) R$$

$$- 2\beta \delta_1 \cos \frac{T}{2} + \delta_1^2 + \beta^2 - \frac{\alpha^2}{4}$$

$$+ \frac{3\alpha\gamma}{4}(v^2 - u^2), \qquad (26)$$

where the $(u^2 + v^2)$ terms were replaced with R. The $(v^2 - u^2)$ term is simplified by multiplying the RHS of Equation (15) by v and subtracting from it the RHS of Equation (16) multiplied by u. This calculation gives

$$(v^2 - u^2) = \frac{1}{2\alpha} \left[3\gamma R^2 + 4 \left(\delta_1 - \beta \cos \frac{T}{2} \right) R \right]. \qquad (27)$$

Substituting this expression into Equation (26) yields the following expression for the determinant:

$$\text{Det}(J) = \frac{45}{16}\gamma^2 R^2 - \frac{9}{2}\gamma \left(\beta \cos \frac{T}{2} - \delta_1\right) R$$
$$- 2\beta\delta_1 \cos \frac{T}{2} + \delta_1^2 + \beta^2 - \frac{\alpha^2}{4}. \qquad (28)$$

The value of R at the nontrivial slow flow equilibria are given by Equation (19). Substituting that expression for R into the expression for the determinant, Equation (28), yields the value of the determinant at the slow flow equilibria

$$\text{Det}(J) = -4\beta^2 \sin^2 \frac{T}{2} + \alpha^2$$
$$\pm 2 \left(\beta \cos \frac{T}{2} - \delta_1\right) \sqrt{\alpha^2 - 4\beta^2 \sin^2 \frac{T}{2}}. \qquad (29)$$

A change in stability occurs when the determinant vanishes. Thus, by setting Equation (29) equal to zero, we may solve for a critical value of δ_1, the detuning, as a function of T for a given α and β

$$\delta_1 = \beta \cos \frac{T}{2} \pm \frac{1}{2}\sqrt{\alpha^2 - 4\beta^2 \sin^2 \frac{T}{2}}. \qquad (30)$$

From Equation (19), Equation (30) implies $R = 0$. This means that the stability change associated with Equation (30) occurs at the origin. Accompanying this change in stability is a bifurcation. If the inequalities (21)–(23) are replaced by equal signs, then Equation (21) becomes the condition for a *saddle-node bifurcation* and Equations (22) and (23) become conditions for *pitchfork bifurcations*.

We will illustrate these results by considering two examples.

4 Example 1

We consider the case in which $\beta = \frac{1}{4}$ and $\alpha = \gamma = 1$. Equation (30) for this example becomes

$$\delta_1 = \frac{1}{4} \cos \frac{T}{2} \pm \frac{1}{2}\sqrt{1 - \frac{1}{4} \sin^2 \frac{T}{2}}. \qquad (31)$$
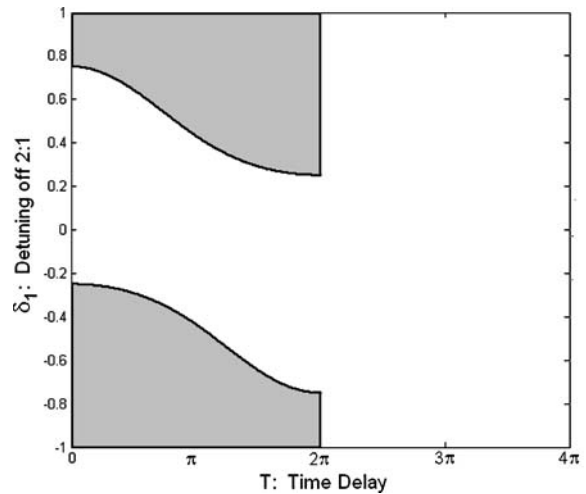

Fig. 4 Stability of the origin for Example 1, $\beta = \frac{1}{4}$ and $\alpha = \gamma = 1$. The transition curves separating the stability regions are given by Equation (31) and by $T = 2\pi$. The solution is stable in the *shaded regions* and unstable in the *unshaded regions*

As stated in the previous section, the origin changes stability along the curves in the $T-\delta_1$ parameter plane given by Equation (31), corresponding to $\text{Det}(J) = 0$. In addition, there is a stability change along the line $T = 2\pi$, corresponding to $\text{Tr}(J) = 0$, when $\text{Det}(J) > 0$. See Fig. 4.

Equation (31) also corresponds to the occurrence of pitchfork bifurcations in the slow flow. These curves are shown in the bifurcation set in Fig. 5. Along with the curves are points labeled with letters from a to i. Each letter corresponds to the qualitative phase portrait of the respective slow flow system as shown in Fig. 6. Pitchfork bifurcations occur as we move from top to bottom in each column of Fig. 6.

As we move from left to right in each row of Fig. 6, we cross the line $T = 2\pi$. For those slow flow equilibria for which $\text{Det}(J) > 0$ (nonsaddles), a stability change is observed, but no limit cycle is seen to be born. The associated Hopf bifurcation turns out to be degenerate, as will be shown later in the paper.

5 Example 2

We consider the case in which $\beta = \frac{3}{5}$ and $\alpha = \gamma = 1$. This example exhibits qualitatively different behavior from the previous example. Equation (30) for this ex-

Fig. 6 Qualitative phase portraits for Example 1, $\beta = \frac{1}{4}$ and $\alpha = \gamma = 1$. The letters a–i correspond to various parameter combinations of δ_1 and T as shown in Fig. 5. Pitchfork bifurcations occur from a to g, b to h, and c to i, respectively. Degenerate Hopf bifurcations occur from a to c, d to f, and g to i, respectively
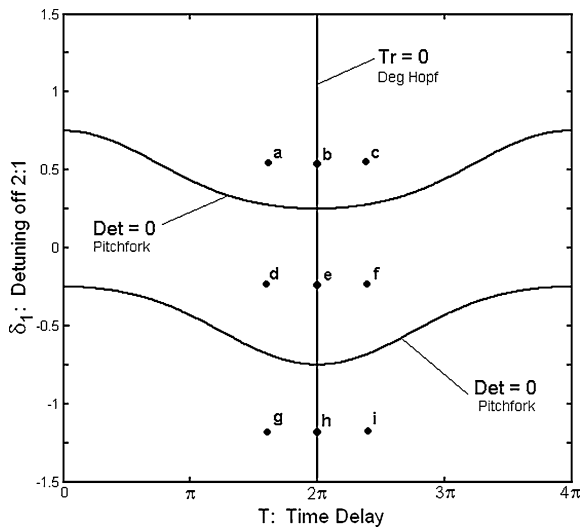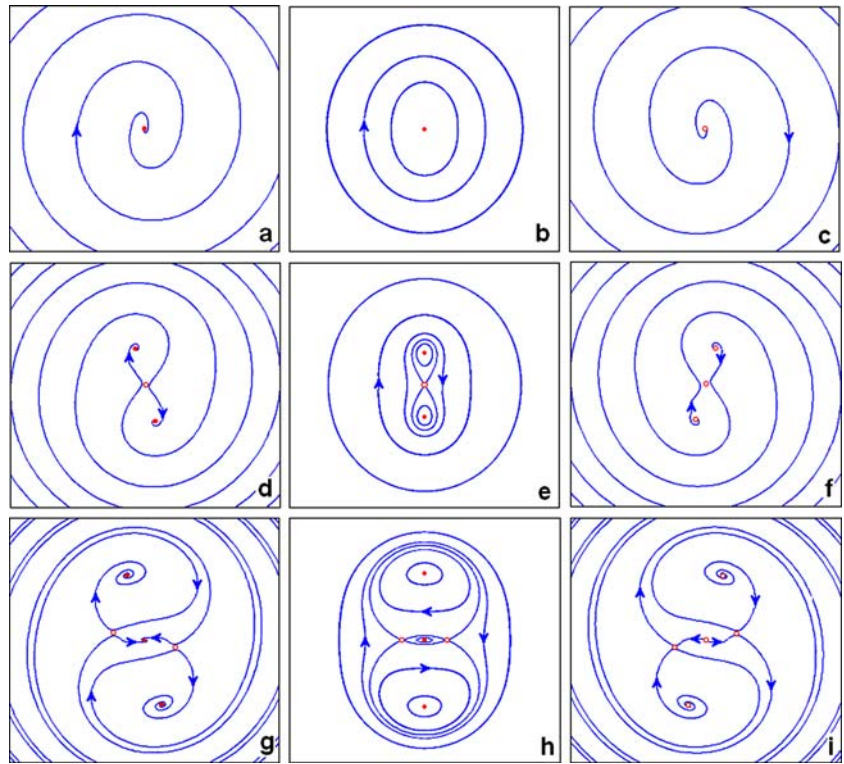

Fig. 5 Bifurcations in slow flow equilibria for Example 1, $\beta = \frac{1}{4}$ and $\alpha = \gamma = 1$. The letters a–i correspond to the qualitative phase portraits shown in Fig. 6. Pitchfork bifurcations occur on the $\text{Det}(J) = 0$ curves, given by Equation (31). A change of stability occurs on the $\text{Tr}(J) = 0$ curve, $T = 2\pi$, in the case that $\text{Det}(J) > 0$ (nonsaddle equilibria). No limit cycles are observed to be born as we cross the latter curve because the associated Hopf bifurcation is degenerate
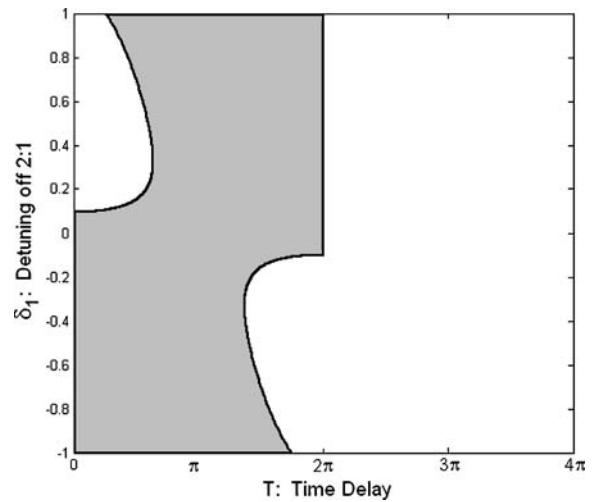
Fig. 7 Stability of the origin for Example 2, $\beta = \frac{3}{5}$ and $\alpha = \gamma = 1$. The transition curves separating the stability regions are given by Equation (32) and by $T = 2\pi$. The solution is stable in the *shaded regions* and unstable in the *unshaded regions*

ample becomes

$$\delta_1 = \frac{3}{5} \cos \frac{T}{2} \pm \frac{1}{2} \sqrt{1 - \frac{36}{25} \sin^2 \frac{T}{2}}. \qquad (32)$$
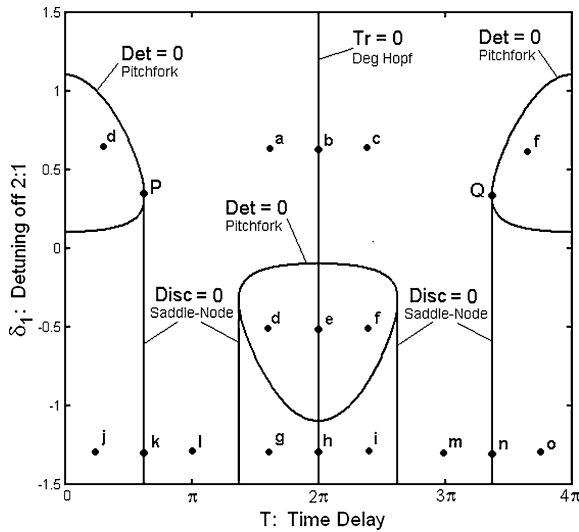
Fig. 8 Bifurcations in slow flow equilibria for Example 2, $\beta = \frac{3}{5}$ and $\alpha = \gamma = 1$. The letters a–i correspond to the qualitative phase portraits shown in Fig. 6. The letters j–o correspond to the qualitative phase portraits shown in Fig. 9. Pitchfork bifurcations occur on the $\text{Det}(J) = 0$ curves, given by Equation (32). Saddle-node bifurcations occur on the $Disc = 0$ curves, given by $|\sin(T/2)| = 5/6$. A change of stability occurs on the $\text{Tr}(J) = 0$ curve, $T = 2\pi$, in the case that $\text{Det}(J) > 0$ (nonsaddle equilibria). No limit cycles are observed to be born as we cross the latter curve because the associated Hopf bifurcation is degenerate

Figure 7 shows the curves (32), corresponding to $\text{Det}(J) = 0$, which bound the stability regions of the origin. In addition, there is a stability change along the line $T = 2\pi$, corresponding to $\text{Tr}(J) = 0$, when $\text{Det}(J) > 0$. Note that for this example, when $|\sin(T/2)| > 5/6$ the discriminant in Equation (32) is less than zero, resulting in a complex conjugate pair. Therefore, it is possible to eliminate the regions of instability by choosing the time delay T appropriately.

Equation (32) also corresponds to the occurrence of pitchfork bifurcations in the slow flow. These curves are shown in the bifurcation set in Fig. 8. The curve $T = 2\pi$ is also shown in Fig. 8, representing a degenerate Hopf in which no limit cycle is born, as in Example 1. In addition, saddle-node bifurcations occur in Example 2 corresponding to the vanishing of the discriminant in Equation (32). These occur when $|\sin(T/2)| = 5/6$, and appear as vertical lines marked $Disc = 0$ in Fig. 8.

Along with these bifurcation curves are points labeled with letters from a to o. Each letter corresponds to the qualitative phase portrait of the corresponding slow flow. The points a through i are qualitatively the same as in Fig. 6. The points j through o are shown

in Fig. 9. Saddle-node bifurcations occur as we move from left to right in each row of Fig. 9.

6 Degenerate HOPF bifurcation

Limit cycles can be generically created or destroyed in a Hopf bifurcation. The necessary conditions for a generic Hopf bifurcation in a system of two first-order ODEs such as the slow flow (15) and (16) are $\text{Tr}(J) = 0$ and $\text{Det}(J) > 0$, where J is the Jacobian matrix evaluated at an equilibrium point. Setting the trace equal to zero in Equation (25) for the slow flow gives $T = 2\pi$ (we ignore $\beta = T = 0$ because the corresponding systems involve no delay). The condition $\text{Det}(J) > 0$ corresponds to a nonsaddle equilibrium point. Thus, if we were to increase the time delay T through 2π, we would expect to see a limit cycle created or destroyed (depending upon whether the Hopf was subcritical or supercritical) in the neighborhood of a spiral equilibrium point. This is shown in Fig. 6 where moving from a to c, from d to f, or from g to i corresponds to increasing the time delay T through 2π. By inspection, no limit cycle is observed, which is contrary to our expectations.

In order to understand this behavior, we evaluate the slow flow (15) and (16) at $T = 2\pi$

$$u' = \left(\delta_1 - \frac{\alpha}{2} + \beta\right)v + \frac{3\gamma}{4}v(u^2 + v^2) \tag{33}$$

$$v' = \left(-\delta_1 - \frac{\alpha}{2} - \beta\right)u - \frac{3\gamma}{4}u(u^2 + v^2). \tag{34}$$

Equations (33) and (34) possess the following first integral

$$\frac{3\gamma}{4}(u^2 + v^2)^2 + 2(\delta_1 + \beta)(u^2 + v^2)$$
$$+ \alpha(u^2 - v^2) = \text{constant}. \tag{35}$$

Note that the existence of this first integral for $T = 2\pi$ is in agreement with the phase portraits b, e, and h in Fig. 6, which were obtained by numercial integration.

In a generic Hopf bifurcation, the limit cycle is born with zero amplitude and grows generically like $\sqrt{\mu}$, where μ is the bifurcation parameter. This results in a family of limit cycles, one for each value of μ. What has happened in the slow flow (15) and (16) is that the entire family of periodic motions has occurred at $\mu = 0$, which corresponds to $T = 2\pi$ here. The

Hopf bifurcation in this case is degenerate. This phenomenon is well-known [13], and a condition has been given that guarantees that no such degeneracy will occur, namely that the equilibrium point should be a "vague attractor" (or less generally, asymptotically stable) when $\mu = 0$. Since the slow flow (15) and (16) has just been shown to be conservative at $T = 2\pi$, this condition does not apply.

Having established that the Hopf bifurcation associated with the slow flow (15) and (16) is degenerate, we are led to ask if this nongeneric behavior is really part of the dynamics of the original Equation (1), or if it is due to the nature of the perturbation scheme. In order to investigate this possibility, we apply an alternative perturbation scheme to Equation (1), based on taking ε small in the following equation

$$\ddot{x}(t) + \delta_0 x(t) - bx(t - T)$$
$$= -\varepsilon(\delta_1 x(t) + \alpha x(t) \cos t + \gamma x(t)^3). \quad (36)$$

We treat this equation in the Appendix, where we use multiple time scales to obtain a slow flow, which we show also exhibits a degenerate Hopf bifurcation.

Further evidence of the existence of the degenerate Hopf in the original Equation (1) was obtained by numerically integrating Equation (1) in the neighborhood of $T = 2\pi$ for a variety of other parameters. Since a limit cycle in the slow flow corresponds to a quasiperiodic motion in the original equation, we searched for quasiperiodic motions in

Equation (1). No quasiperiodic motions were observed.

7 Comparison with numerical integration

In this section, we compare the foregoing analytical results based on the slow flow (13) and (14) or (15) and (16), with direct numerical integration of the delayed Mathieu Equation (2). The numerical integration was completed in MATLAB, which has recently extended the differential equation package to numerically integrate systems of delay differential equations [14]. For this task, we used the integrating function dd23. There is a tutorial available at MATLAB Central Website [15].

The results presented are for the stability of the origin, $x = \dot{x} = 0$, and are shown in Figs. 10 and 11. We used the same parameters that were used in Examples 1 and 2, except we took $\gamma = 0$, since the stability of the origin does not involve the nonlinear term in Equation (2). In particular, we used $\beta = 0.25$ in Fig. 10 and $\beta = 0.60$ in Fig. 11. A MATLAB script was written to generate these figures numerically, utilizing the dd23 function. The $T-\delta_1$ parameter plane was divided into a grid of 10,000 points. A point in this space was deemed stable if, after 2000 forcing periods starting with the initial condition $x = 1$, the norm of the amplitude is less than 10^{10}, otherwise it was unstable. For each figure, $\varepsilon = 0.05$.

In Fig. 10, we note the appearance of a stable region on the right side of the numerical (lower) stability chart that is absent from the analytical (upper) stability chart. This may be explained by recalling that the analytical

Fig. 9 Qualitative phase portraits for Example 2, $\beta = \frac{3}{5}$ and $\alpha = \gamma = 1$. The letters j–o correspond to various parameter combinations of δ_1 and T as shown in Fig. 8. Saddle-node bifurcations occur from j to l and from m to o, respectively
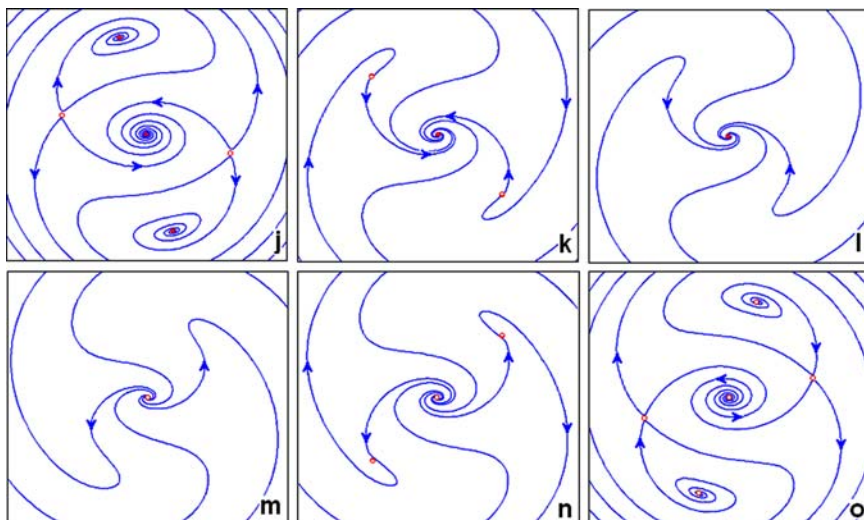
Fig. 10 Stability of the origin for $\beta = 0.25$ and $\alpha = 1$. Comparison between analytical results based on slow flow (*upper*) with numerical integration of Equation (2) for $\varepsilon = 0.05$ (*lower*). The solution is stable in the *shaded regions* and unstable in the *unshaded regions*
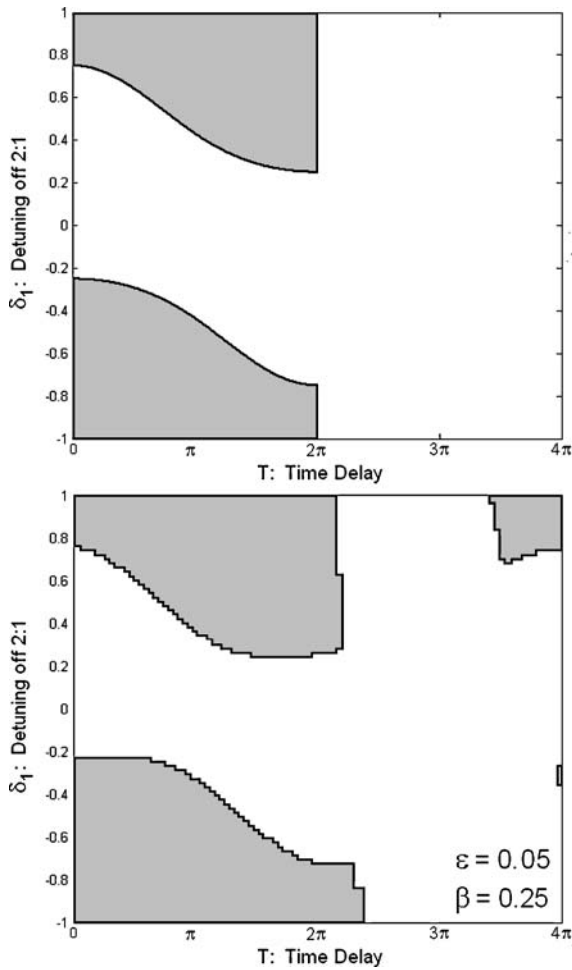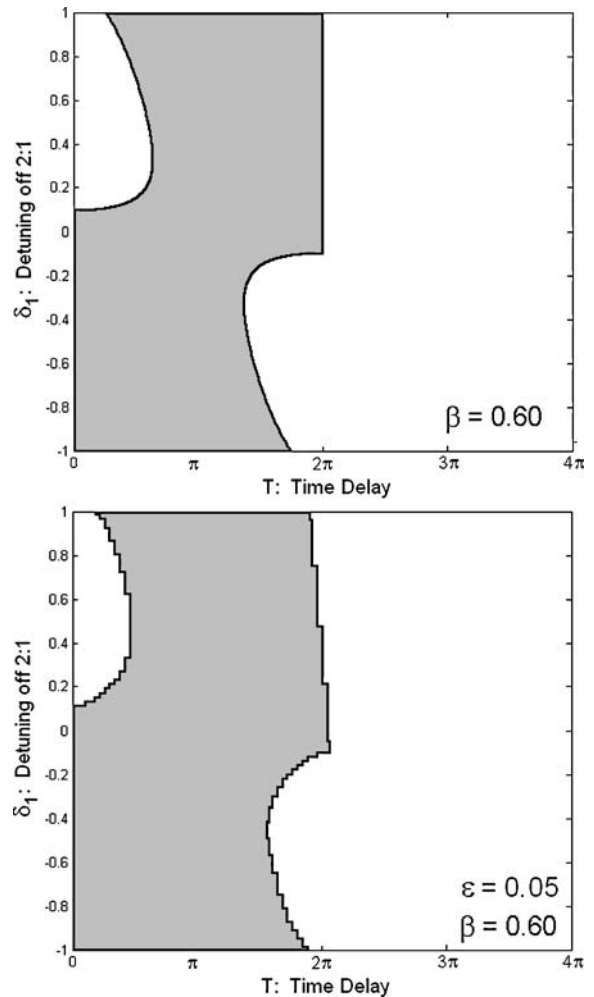
Fig. 11 Stability of the origin for $\beta = 0.60$ and $\alpha = 1$. Comparison between analytical results based on slow flow (*upper*) with numerical integration of Equation (2) for $\varepsilon = 0.05$ (*lower*). The solution is stable in the *shaded regions* and unstable in the *unshaded regions*

results are based on a perturbation method that assumed that εT was small.

8 Discussion

The main difference between Examples 1 and 2 presented earlier in this paper is that Example 2 involves a saddle-node bifurcation and Example 1 does not. The saddle-node bifurcation occurs because the condition for nontrivial slow flow equilibria to exist, Equation (21), is not satisfied for all values of T. Recall that the instability region in the $T–\delta_1$ parameter plane was bounded by curves with Equations (22) and (23). Thus, for each time delay T, and for given values of α

and β, there are two critical values of δ_1 if $\beta < \alpha/2$. If $\beta > \alpha/2$, however, there are values of T for which there are no real critical values of δ_1, and therefore there is no instability.

Recalling that $\delta = 1/4 + \delta_1\varepsilon$, we may write the transition curves separating stable from unstable regions in the form

$$\delta = \frac{1}{4} + \varepsilon\left(\beta\cos\frac{T}{2} \pm \frac{1}{2}\sqrt{\alpha^2 - 4\beta^2\sin^2\frac{T}{2}}\right) \quad (37)$$

Figure 12 shows the instability region (37) in the three-dimensional $\delta–T–\varepsilon$ parameter space for the parameters

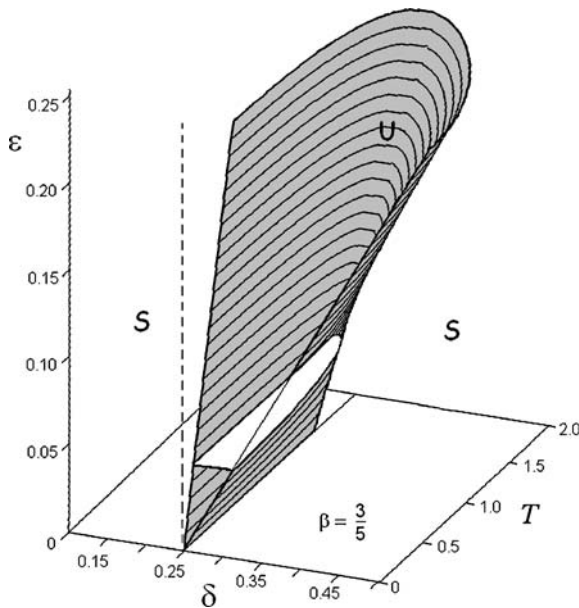$\underline{\textcircled{2}}$ Springer

Fig. 12 The 2:1 instability tongue, Equation (37), for $\beta = \frac{3}{5}$, $\alpha = \gamma = 1$. S: stable, U: unstable. The *white instability region* lying in the plane $\varepsilon = 0.05$ corresponds to the *white instability region* on the *left side* of Fig. 11
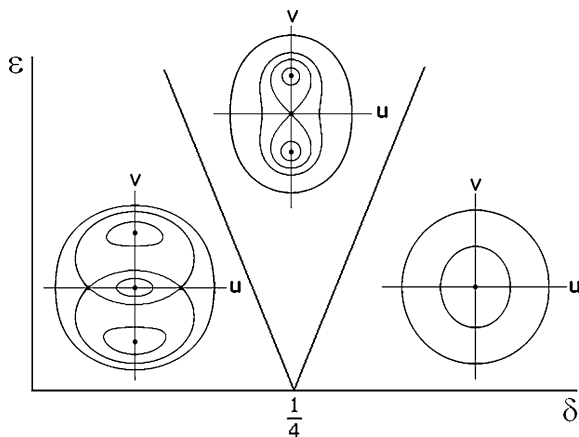

Fig. 13 Bifurcation diagram for the nonlinear Mathieu equation without delay term, Equation (1) with $\alpha = \gamma = 1$, $\beta = 0$

of Example 2. Figure 12 can be compared with Fig. 11 by intersecting the three-dimensional instability tongue with the plane $\varepsilon = 0.05$. Thus, the white region lying inside the tongue in Fig. 12 is the same as the white instability region on the left side of Fig. 11.

In the limiting case of $\beta = 0$ (no delay), Equation (1) becomes a nonlinear Mathieu equation, the properties of which are well-known [4]. Figure 13 displays a bifurcation diagram for Equation (1) with $\alpha = \gamma = 1$, $\beta = 0$. The effect of adding a small delay term may

be understood by perusing Figs. 5 and 6. These show, first of all, that the presence of delay introduces dissipation into the slow flow. Moreover, we see that if the delay amplitude β is small enough ($0 < \beta < \alpha/2$), and if the time delay T is small enough ($T < 2\pi$), then the dynamics of the delayed equation is similar to that of a damped nonlinear Mathieu equation without delay. However, if the delay amplitude is large enough ($\beta > \alpha/2$), then we showed that it is possible to eliminate the tongue of instability by choosing the time delay appropriately. The minimum time delay required is $T = 2\sin^{-1}\frac{\alpha}{2\beta}$. See Figs. 8 and 9.

The stability change at the origin is given by Equation (30). This equation can be rewritten so as to give the following condition for instability at the origin

$$\delta_1^2 + \beta^2 - 2\beta\delta_1 \cos\frac{T}{2} - \frac{\alpha^2}{4} < 0. \qquad (38)$$

This shows that the origin is unstable for all time delays T if the delay amplitude β and the detuning δ_1 are taken to be sufficiently small. For example, in Fig. 4, where $\beta = 1/4$, the origin is always unstable for $|\delta_1| < 1/4$.

9 Conclusions

In this paper, we investigated the dynamics of Equation (1) that involves the interaction of parametric excitation with delay. Our analytical results are based on slow flow Equations (15) and (16) that were obtained using first-order averaging. We studied the stability of the origin and the bifurcations that accompanied stability changes: pitchforks, saddle-nodes, and degenerate Hopf bifurcations.

We showed that adding delay to an undamped parametrically excited system may introduce effective damping. Our most important conclusion is that for sufficiently large delay amplitudes β, and for appropriately chosen time delays T, the 2:1 instability region associated with parametric excitation can be eliminated. This result has potential utility in engineering applications where instabilities are undesirable. For example, Masoud and Nayfeh conclude that time delay reduces the swaying of container cranes [16].

Appendix

The occurrence of a degenerate bifurcation in a slow flow system derived from a perturbation method may not be representative of the actual system. The degeneracy may result from the approximation involved in the perturbation method. The slow flow system (15) and (16) in the previous section was derived by perturbing off of a simple harmonic oscillator with $O(\varepsilon)$ forcing, nonlinearity, detuning, and delay (Cf. Equation (2)):

$$
\ddot{x}(t) + \delta_0 x(t) = -\varepsilon(\delta_1 x(t) + \alpha x(t) \cos t \\
+ \gamma x(t)^3 - \beta x(t - T)).
\tag{A.1}
$$

An alternative approach is to perturb off of the Hsu–Bhatt Equation [5] $\ddot{x} + \delta_0 x = b(t - T)$. We consider a simple harmonic oscillator with a delay term, which is perturbed by $O(\varepsilon)$ forcing, nonlinearity, and detuning

$$
\ddot{x}(t) + \delta_0 x(t) - b x(t - T) \\
= -\varepsilon(\delta_1 x(t) + \alpha x(t) \cos t + \gamma x(t)^3),
\tag{A.2}
$$

where the delay amplitude is b, the time delay is T, and δ_0 is the frequency squared of the simple harmonic oscillator. If the delay amplitude b and ε were zero, then this system would be stable when $\delta_0 > 0$ and unstable when $\delta_0 < 0$. By changing the delay parameters b and T, the stable system can become unstable and the unstable system can become stable. Thus, a change of stability would occur.

The solution to Equation (A.2) is for $\varepsilon = 0$ of the form $x(t) = e^{\lambda t}$, where the characteristic equation is:

$$
\lambda^2 + \delta_0 = b\, e^{-\lambda T}.
\tag{A.3}
$$

Note that Equation (A.3) is a transcendental equation on λ and therefore has an infinite number of (generally complex) roots. For a Hopf bifurcation, the real part of the complex conjugate pair must be zero. Substituting $\lambda = i\omega$ into Equation (A.3) yields

$$
\omega_{\text{crit}}^2 = \delta_0 + b, \quad \omega_{\text{crit}} T_{\text{crit}} = \pi
\tag{A.4}
$$

which gives the solution to the Hsu–Bhatt Equation (A.2) for $\varepsilon = 0$ right at a Hopf bifurcation point. This is the starting point for the perturbation method.

We use the multiple time scales method and begin by perturbing off of the critical value of the time delay

$$
T = T_{\text{crit}} + \varepsilon\mu + \cdots
\tag{A.5}
$$

We then define two time scales $\xi = t$ and $\eta = \varepsilon t$, and expand x in a power series of ε: $x(\xi, \eta) = x_0(\xi, \eta) + \varepsilon x_1(\xi, \eta) + \cdots$ We substitute these expansions into Equation (A.2) and collect like terms. The solution to the $\varepsilon = 0$ equation is

$$
x_0(\xi, \eta) = A_1(\eta) \cos \omega_{\text{crit}} \xi + A_2(\eta) \sin \omega_{\text{crit}} \xi,
\tag{A.6}
$$

where $A_1(\eta)$ and $A_2(\eta)$ are functions of slow time η. In order for the $\cos t$ term in Equation (A.2) to be 2:1 resonant, $\omega_{\text{crit}} = \frac{1}{2}$. This implies from Equation (A.4)

$$
\delta_0 + b = \frac{1}{4}, \quad T_{\text{crit}} = 2\pi + \varepsilon\mu.
\tag{A.7}
$$

The $O(\varepsilon)$ equation is

$$
x_{1\xi\xi} + \delta_0 x_1 - b x_1(\xi - T_{\text{crit}}) \\
= -\big(2x_{0\xi\eta} + (\delta_1 + \alpha \cos \xi)x_0 \\
+ \gamma x_0^3 + \mu x_{0\xi}(\xi - T_{\text{crit}})\big),
\tag{A.8}
$$

where the subscripts denote partial derivatives, $T_{\text{crit}} = 2\pi$, and x_0 is given by Equation (A.6). In deriving Equation (A.8) the product $\varepsilon T_{\text{crit}}$ was assumed to be small [11]. After substituting Equation (A.6) into (A.8), the removal of resonant terms yields the slow flow

$$
\frac{dA_1}{d\eta} = \frac{b\mu}{2} A_1 + \left(\delta_1 - \frac{\alpha}{2}\right) A_2 + \frac{3\gamma}{4} A_2\big(A_1^2 + A_2^2\big)
$$
$$
\tag{A.9}
$$
$$
\frac{dA_2}{d\eta} = \frac{b\mu}{2} A_2 - \left(\delta_1 + \frac{\alpha}{2}\right) A_1 - \frac{3\gamma}{4} A_1\big(A_1^2 + A_2^2\big)
$$
$$
\tag{A.10}
$$

As stated in Section 6 (Degenerate Hopf), the necessary conditions for a generic Hopf bifurcation in a system of two first-order ODEs, such as those shown earlier in Equations (A.9) and (A.10), are $\text{Tr}(J) = 0$ and $\text{Det}(J) > 0$, where J is the Jacobian matrix evaluated at the equilibrium point. The trace and determinant for the slow flow system stated earlier about the origin are

$$
\text{Tr}(J) = b\mu, \quad \text{Det}(J) = \frac{b^2\mu^2}{4} + \delta_1^2 - \frac{\alpha}{4}.
\tag{A.11}
$$

Setting the $\text{Tr}(J) = 0$ gives $b = 0$ (which corresponds to a system with no delay) or $\mu = 0$, which is right at the bifurcation point of $T_{\text{crit}} = 2\pi$. Using $\mu = 0$, the condition for the $\text{Det}(J) > 0$ becomes

$$\delta_1^2 > \frac{\alpha}{4} \Rightarrow |\delta_1| > \frac{\alpha}{2}. \qquad (A.12)$$

Thus, for a given $\alpha > 0$, and choosing $|\delta_1| > \alpha/2$, we would expect a limit cycle to be born as we change μ from negative to positive or positive to negative. However, a limit cycle is not born in this slow flow system, contrary to what we expect. In fact, the slow flow in Equations (A.9) and (A.10) at the bifurcation point of $\mu = 0$ has the first integral

$$\left(6\gamma A_2^2 + 8\delta_1 + 4\alpha\right)\frac{A_1^2}{4} + (8\delta_1 - 4\alpha)\frac{A_2^2}{4}$$
$$+ \frac{3\gamma}{4}\left(A_1^4 + A_2^4\right) = C. \qquad (A.13)$$

The existence of this first integral signifies that the Hopf bifurcation is degenerate, as explained at the end of Section 6.

Thus, both perturbation schemes, one in which the delay amplitude is $O(1)$ and the other in which the delay amplitude is $O(\varepsilon)$, yield slow flow systems which exhibit degenerate Hopf bifurcations.

References

1. Stépán, G., Insperger, T., Szalai, R.: Delay, parametric excitation, and the nonlinear dynamics of cutting processes. Int. J. Bifurcation Chaos **15**, 2783–2798 (2005)
2. Davies, M.A., Pratt, J.R., Dutterer, B.S., Burns, T.J.: Stability prediction for low radial immersion milling. ASME J. Manuf. Sci. Eng. **124**, 217–225 (2002)
3. Insperger, T., Stépán, G.: Vibration frequencies in high-speed milling processes, or a positive answer to Davies, Pratt, Dutterer, and Burn. J. Manuf. Sci. Eng. **126**, 481–487 (2004)
4. Rand, R.H.: Lecture Notes on Nonlinear Vibrations, vol. 52. Available at: http://www.tam.cornell.edu/randdocs/nlvibe52.pdf (2005)
5. Bhatt, S.J., Hsu, C.S.: Stability criteria for second-order dynamical systems with time lag. J. Appl. Mech. **33E**, 113–118 (1966)
6. Insperger, T., Stépán, G.: Stability chart for the delayed Mathieu equation. R. Math. Phys. Eng. Sci. **458**, 1989–1998 (2002)
7. Wahi, P., Chatterjee, A.: Averaging oscillations with small fractional damping and delayed terms. Nonlinear Dyn. **38**, 3–22 (2004)
8. Breda, D., Maset, S., Vermiglio, R.: Efficient computation of stability charts for linear time delay systems. In: Proceeding of the 21st ASME International Design Engineering Technology Conference, Long Beach, CA, pp. 24–28 (2005)
9. Insperger, T., Stépán, G.: Updated semi-discretization method for periodic delay-differentilal equations with discrete delay. Int. J. Numer. Methods Eng. **61**, 117–14 (2004)
10. Rand, R.H.: Topics in Nonlinear Dynamics with Computer Algebra. Gordon and Breach, London (1994)
11. Wirkus, S., Rand, R.H.: Dynamics of two coupled van der pol oscillators with delay coupling. Nonlinear Dyn. **30**, 205–221 (2002)
12. Strogatz, S.H.: Nonlinear Dynamics and Chaos. Addison-Wesley, Reading, MA (1994)
13. Marsden, J.E., McCracken, M.: The Hopf Bifurcation and its Applications. Springer, Berlin, Heidelberg, New York (1976)
14. Shampine, L.F., Thompson, S.: Solving delay differential equations in MATLAB. Appl. Numer. Math. **37**, 441–458 (2001)
15. Kierzenka, J.: Solving Delay Differential Equations with dde23. Available at: MATLAB Central. http://www.radford.edu/~thompson/webddes/tutorial.pdf (2003)
16. Masoud, Z.N., Nayfeh, A.H.: Sway reduction on container cranes using delayed feedback control. Nonlinear Dyn. **34**, 347–358 (2003)